

LHC diphoton Higgs signal and top quark forward-backward asymmetry in quasi-inert Higgs doublet model

Lei Wang, Xiao-Fang Han

Department of Physics, Yantai University, Yantai 264005, China

Abstract

In the quasi-inert Higgs doublet model, we study the LHC diphoton rate for a standard model-like Higgs boson and the top quark forward-backward asymmetry at Tevatron. Taking into account the constraints from the vacuum stability, unitarity, electroweak precision tests, flavor physics and the related experimental data of top quark, we find that compared with the standard model prediction, the diphoton rate of Higgs boson at LHC can be enhanced due to the light charged Higgs contributions, while the measurement of the top quark forward-backward asymmetry at Tevatron can be explained to within 1σ due to the non-standard model neutral Higgs bosons contributions. Finally, the correlations between the two observables are discussed.

PACS numbers: 14.65.Ha,14.80.Bn,14.80.Ec,14.80.Fd

I. INTRODUCTION

LHC [1–3] has recently reported some hints for a 125 GeV Higgs boson decaying into two photons and the diphoton rate should be larger than the standard model (SM) one. Due to the absence of a true signal, the expected exclusion limit at 95% confidence level is between 1.4 and 2.4 times the SM rate in the mass range 110-150 GeV from the CMS collaboration [2] and between 1.6 and 1.7 times in the mass range 115-130 GeV from ATLAS collaboration [3]. The LHC diphoton signal has been studied in various extensions of the SM, such as the minimal supersymmetric standard model (MSSM) [4], the two Higgs doublet model [5], the inert Higgs doublet model [6], the next-to-MSSM [7], the little Higgs models [8], the Higgs triplet models [9] and the models with extra dimension [10].

The forward-backward asymmetry A_{FB}^t in top quark pair production has been measured by two experimental groups at the Tevatron. The CDF measured the asymmetry in the $\ell + j$ channel and obtained $A_{FB}^t(CDF) = 0.158 \pm 0.074$ [11], which is nearly consistent with the D0 result $A_{FB}^t(D0) = 0.19 \pm 0.065$ [12]. These results exceed the NLO SM prediction, $A_{FB}^t(SM) = 0.058 \pm 0.009$ [13]. The CDF also reported an anomaly large value of A_{FB}^t for $m_{t\bar{t}} > 450$ GeV [14], which, however, is not confirmed by D0 collaboration [12]. Therefore, we do not consider the experimental data in this paper. To explain A_{FB}^t , various attempts have been tried, such as via the s -channel exchange of an axi-gluon [15] or the t -channel exchange of Z' , W' and a scalar [16–20].

The quasi-inert Higgs doublet model (QIHDM) [21] is proposed by Qing-Hong Cao et al. with the motivation of explaining the excess of Wjj reported by CDF [22]. In addition to the SM particle content, just one complex electroweak scalar doublet is introduced with an approximate Z_2 -symmetry being imposed. This model predicts the SM-like Higgs boson h , the charged Higgs boson H^\pm as well as two neutral Higgs bosons S and A . The three new Higgs bosons can contribute to the diphoton rate of h and the top quark forward-backward asymmetry at Tevatron. Since D0 collaboration does not confirm the excess of Wjj reported by CDF [23], we will not discuss the experimental result of Wjj in this paper.

This work is organized as follows. In Sec. II, we briefly review the quasi-inert Higgs doublet model. In Sec. III, we discuss the relevant theoretical and experimental constraints. In Sec. IV, we study diphoton rate for the SM-like Higgs boson at LHC. In Sec. V, we study the top quark forward-backward asymmetry A_{FB}^t at Tevatron and the correlation between

A_{FB}^t and the LHC diphoton Higgs signal. Finally, we give our conclusion in Sec. VI.

II. QUASI-INERT HIGGS DOUBLET MODEL

The quasi-inert Higgs doublet model is a simple extension of SM by including an additional scalar doublet $\Phi_2 = [H^+, (S + iA)/\sqrt{2}]$, with the same hypercharge as the SM doublet $\Phi_1 = (\phi^+, \phi^0)$. To explicitly forbid the mixing between the two Higgs doublets, we can impose a Z_2 -symmetry under which Φ_2 and Φ_1 are respectively odd and even. The renormalizable scalar potential can be written as [21]

$$V = \mu_1^2 \Phi_1^\dagger \Phi_1 + \mu_2^2 \Phi_2^\dagger \Phi_2 + \lambda_1 \left(\Phi_1^\dagger \Phi_1 \right)^2 + \lambda_2 \left(\Phi_2^\dagger \Phi_2 \right)^2 + \lambda_3 \left(\Phi_1^\dagger \Phi_1 \right) \left(\Phi_2^\dagger \Phi_2 \right) + \lambda_4 \left(\Phi_1^\dagger \Phi_2 \right) \left(\Phi_2^\dagger \Phi_1 \right) + \frac{1}{2} \lambda_5 \left(\Phi_1^\dagger \Phi_2 \right)^2 + \frac{1}{2} \lambda_5^* \left(\Phi_2^\dagger \Phi_1 \right)^2, \quad (1)$$

All the above parameters are necessarily real except λ_5 . The SM $SU(2) \times U(1)_Y$ gauge symmetry is spontaneously broken by the vacuum expectation value (VEV) of ϕ^0 field, $\langle \phi^0 \rangle = v = 246 \text{ GeV}$. Φ_2 field does not develop VEV from Eq. (1).

The quartic coupling λ_i can be expressed by the physical scalar masses and μ_2 as follow:

$$\lambda_1 = \frac{m_h^2}{2v^2}, \quad \lambda_3 = \frac{2}{v^2} (m_{H^\pm}^2 - \mu_2^2), \\ \lambda_4 = \frac{(m_S^2 + m_A^2 - 2m_{H^\pm}^2)}{v^2}, \quad \lambda_5 = \frac{(m_S^2 - m_A^2)}{v^2} \quad (2)$$

The scalar potential in Eq. (1) contains the SM-like Higgs boson coupling with the charged Higgs,

$$g_{hH^\pm H^\mp} = -i\lambda_3 v = -i \frac{2m_{H^\pm}^2}{v} \left(\frac{m_{H^\pm}^2 - \mu_2^2}{m_{H^\pm}^2} \right). \quad (3)$$

In order to explain the top quark forward-backward asymmetry at Tevatron, Φ_2 field has to couple to the first generation quark. Therefore, we require the right-handed up quark is odd under Z_2 -symmetry, while all the other SM fields are even. Thus, the Yukawa couplings of the quark fields can be written as [21]

$$\mathcal{L}_Y = -y_{u,1}^{ik} \bar{Q}_L^i \tau_2 \Phi_1^* u_R^k - y_{d,1}^{ij} \bar{Q}_L^i \Phi_1 d_R^j - y_{u,2}^{i1} \bar{Q}_L^i \tau_2 \Phi_2^* u_R^1 + h.c., \quad (4)$$

where $\tau_2 = i\sigma_2$ (σ_2 is Pauli matrix) and $Q_L^i = (u_L^i, d_L^i)^T$. The generation indices i, j run from 1 to 3, and k can only takes 2 and 3. The coupling of the right-handed up quark to Φ_1 is forbidden by the Z_2 -symmetry, which leads that the up quark remains massless at

tree-level. In order to generate the up quark mass, a soft breakdown scalar potential of the Z_2 -symmetry, $\mu_{12}^2 \Phi_1^\dagger \Phi_2 + h.c.$, is necessary. Since the up quark mass is about a few MeV, μ_{12}^2 is relative small, which can induce a negligible VEV of Φ_2 field compared with that of Φ_1 field.

In the mass eigenstates, we can obtain the coupling of the right-handed up quark to Φ_2 field from Eq. (4),

$$\mathcal{L}_u = - \frac{S - iA}{\sqrt{2}} (X_u)^{i1} \bar{u}_L^i u_R^1 + H^- (V_{CKM}^\dagger X_u)^{i1} \bar{d}_L^i u_R^1 + h.c., \quad (5)$$

where $(X_u)^{i1} = (U_{u,L}^\dagger)^{ij} (y_{u,2})^{j1}$ with $U_{u,L}$ being the rotation matrix of the left-handed up-type quarks. We choose to make the simplifying assumption, $(U_{u,L})^{ij} = \delta^{ij}$.

To explain the top quark forward-backward asymmetry and satisfy the constraints from the flavor processes, we take

$$(X_u)^{i1} = 2y_1 (V_{CKM})^{i3}. \quad (6)$$

The detailed analysis was given in [18]. Where $y_1 = \frac{1}{2}(y_{u,2})^{i1}/(V_{CKM})^{i3}$ for $(U_{u,L})^{ij} = \delta^{ij}$. From the Eq. (5), we can get the coupling

$$\mathcal{L}_u = -2y_1 \left((V_{CKM})^{i3} \frac{S - iA}{\sqrt{2}} \bar{u}_L^i u_R^1 - H^- \bar{b}_L u_R^1 \right) + h.c.. \quad (7)$$

In the quasi-inert Higgs doublet model, both S and A couple to the up quark, which leads that they are no longer the candidate for dark matter. To provide a candidate for dark matter, a possible approach is to introduce a single scalar field with an extra discrete symmetry being imposed, which will be studied elsewhere.

III. THEORETICAL AND EXPERIMENTAL CONSTRAINTS

• **$D - \bar{D}$ mixing and same-sign top pair production at LHC:** The couplings of S and A to up quark in Eq. (7) can contribute to the $D - \bar{D}$ mixing and the same-sign top pair production at LHC [21, 24]. The contributions of S and A are destructive and such contributions can be canceled for degenerate S and A masses. Therefore, in this paper, we take $m_S = m_A$, which implies $\lambda_5 = 0$ from the Eq. (2).

•**Electroweak precision tests:** The electroweak S and T parameters can give the constraints on the splitting of the charged Higgs and the neutral Higgs masses [18, 21].

Considering the LEP constraints [25], we take $m_{H^\pm} = m_S = m_A \geq 90$ GeV, which implies $\lambda_4 = 0$ from the Eq. (2).

•**Vacuum stability and unitarity:** For $m_{H^\pm} = m_S = m_A$, the vacuum stability can give the constraints on the parameters [26]:

$$\lambda_{1,2} > 0, \quad \lambda_3 > -2\sqrt{\lambda_1\lambda_2}. \quad (8)$$

The unitarity constraints for the scalar potential were calculated in Ref. [6, 27]. Various processes were used to constrain quartic couplings at the tree level. These lead to a set of unitarity constrained parameters:

$$\begin{aligned} e_{1,2} &= \lambda_3 \pm \lambda_4 \quad , \quad e_{3,4} = \lambda_3 \pm \lambda_5 \\ e_{5,6} &= \lambda_3 + 2\lambda_4 \pm 3\lambda_5 \quad , \quad e_{7,8} = -\lambda_1 - \lambda_2 \pm \sqrt{(\lambda_1 - \lambda_2)^2 + \lambda_4^2} \\ e_{9,10} &= -3\lambda_1 - 3\lambda_2 \pm \sqrt{9(\lambda_1 - \lambda_2)^2 + (2\lambda_3 + \lambda_4)^2} \\ e_{11,12} &= -\lambda_1 - \lambda_2 \pm \sqrt{(\lambda_1 - \lambda_2)^2 + \lambda_5^2}. \end{aligned}$$

The absolute values of the twelve parameters must be smaller than 8π . The strongest constraint on $\lambda_{1,2}$ comes from $e_{9,10}$, which gives approximately [6]:

$$\lambda_1 + \lambda_2 < \frac{8\pi}{3}. \quad (9)$$

The coupling λ_1 can be determined by the Higgs mass m_h from the Eq. (2). Requiring the absolute values of e_i ($i = 1, \dots, 12$) to be smaller than 8π and the Eq. (8) to be satisfied, we can get the lower bound of λ_3 for a fixed m_h and $m_{H^\pm} = m_S = m_A$. For $m_h = 120$ GeV, 125 GeV and 130 GeV (*i. e.* $\lambda_1 = 0.12, 0.13, 0.14$), the lower bound of λ_3 is respectively -1.4, -1.45 and -1.5.

•**The $t\bar{t}$ total production cross sections and $t\bar{t}$ invariant mass distribution at the Tevatron:** The current cross section measured at Tevatron is $\sigma^{exp} = 7.50 \pm 0.48$ pb for $m_t = 172.5$ GeV [28], while the SM cross section is $\sigma^{SM} = 7.46_{-0.80}^{+0.66}$ pb from [29] and $\sigma^{SM} = 6.30 \pm 0.19_{-0.23}^{+0.31}$ pb from [30]. Here, we conservatively require $-0.12 < \frac{\sigma^{NP}}{\sigma^{SM}} < 0.3$ for the Tevatron. The invariant mass distribution was also measured by CDF, and the results are presented in nine bins of $M_{t\bar{t}}$ [31]. We require the differential cross section in each bin to be within the 2σ regions of their experimental values. In this paper, the mass of top quark is taken as 172.5 GeV.

•**New top quark decay channels:** The top quark can decay into a light quark and a scalar particle for the scalar mass is light enough. The measurement of the total top quark width is $\Gamma_t^{exp} = 1.99_{-0.55}^{+0.69}$ GeV [32], which is in agreement with the SM value $\Gamma_t^{SM} = 1.3$ GeV. We require the total top quark width to be within the 2σ regions of the experimental value.

The flavor changing couplings in the Eq. (7) can contribute to the single top quark production through the $gu \rightarrow tS$ (A) process. The D0 has recently measured single top quark production cross section at the Tevatron and obtained $\sigma(p\bar{p} \rightarrow tqb + X) = 2.90 \pm 0.59$ pb [33]. However, the single top quark production data gives no constraints to this model because of the difference between final states in experiments and those in this model.

IV. DIPHOTON RATE FOR A 120 – 130 GEV HIGGS AT THE LHC

In our calculations, we take $m_{H^\pm} = m_S = m_A = m_2 \geq 90$ GeV, so the decays into these Higgs bosons are kinematically forbidden for a light SM-like Higgs boson h . Except for the decay $h \rightarrow \gamma\gamma$, the decay modes and their widths of the SM-like Higgs boson are the same both in QIHDM and SM. Since the decay width of $h \rightarrow \gamma\gamma$ is very small, the total width of SM-like Higgs boson in QIHDM almost equals to that in SM.

In the SM, the decay $h \rightarrow \gamma\gamma$ is dominated by the W loop which can also interfere destructively with the subdominant top quark loop. In QIHDM, the charged Higgs boson H^\pm loop can give the additional contributions to the the decay width $\Gamma(h \rightarrow \gamma\gamma)$, which can be expressed as [34]

$$\Gamma(h \rightarrow \gamma\gamma) = \frac{\alpha^2 m_h^3}{256\pi^3 v^2} \left| \sum_i N_{ci} Q_i^2 F_{1/2}(\tau_f) + F_1(\tau_W) + g_{H^\pm} F_0(\tau_{H^\pm}) \right|^2, \quad (10)$$

where

$$g_{H^\pm} = \frac{\lambda_3 v^2}{2m_{H^\pm}^2} = \frac{m_{H^\pm}^2 - \mu_2^2}{m_{H^\pm}^2}, \quad \tau_f = \frac{4m_f^2}{m_h^2}, \quad \tau_W = \frac{4m_W^2}{m_h^2}, \quad \tau_{H^\pm} = \frac{4m_{H^\pm}^2}{m_h^2}. \quad (11)$$

N_{ci} , Q_i are the color factor and the electric charge respectively for fermion i running in the loop. The dimensionless loop factors for particles of spin given in the subscript are:

$$F_1 = 2 + 3\tau + 3\tau(2 - \tau)f(\tau), \quad F_{1/2} = -2\tau[1 + (1 - \tau)f(\tau)], \quad F_0 = \tau[1 - \tau f(\tau)], \quad (12)$$

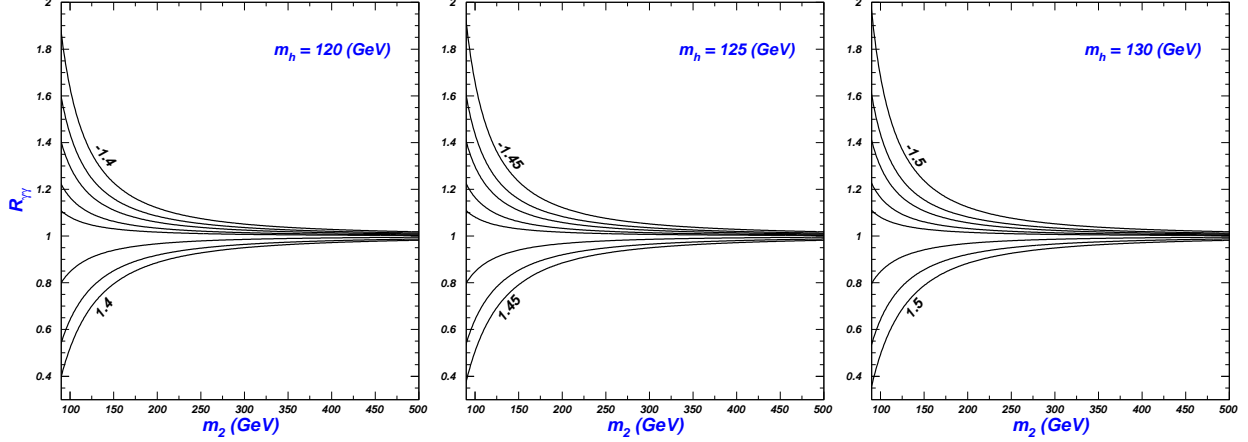


FIG. 1: The $R_{\gamma\gamma}$ versus the H^\pm mass (m_2) for several different λ_3 . For the left (middle, right) panel, $m_h = 120$ (125, 130) GeV and the curves from bottom to top correspond to $\lambda_3 = 1.4$ (1.45, 1.5), 1.0, 0.4, -0.2, -0.4, -0.7, -1.0, -1.4 (-1.45, 1.5).

with

$$f(\tau) = \begin{cases} [\sin^{-1}(1/\sqrt{\tau})]^2, & \tau \geq 1 \\ -\frac{1}{4}[\ln(\eta_+/\eta_-) - i\pi]^2, & \tau < 1 \end{cases} \quad (13)$$

where $\eta_\pm = 1 \pm \sqrt{1 - \tau}$.

The Higgs boson production cross section at the LHC are the same both in the QIHDM and SM. Therefore, the LHC diphoton rate of Higgs boson in the QIHDM normalized to the SM prediction can be written as

$$R_{\gamma\gamma} = \frac{Br(h \rightarrow \gamma\gamma)}{Br(h \rightarrow \gamma\gamma)^{SM}} \simeq \frac{\Gamma(h \rightarrow \gamma\gamma)}{\Gamma(h \rightarrow \gamma\gamma)^{SM}}. \quad (14)$$

In Fig. 1 we show the $R_{\gamma\gamma}$ versus the H^\pm mass (m_2) for several different λ_3 . Fig. 1 shows $R_{\gamma\gamma}$ is almost the same for $m_h = 120$ GeV, 125 GeV and 130 GeV. H^\pm contributions can interfere constructively for $\lambda_3 < 0$ and interfere destructively for $\lambda_3 > 0$, leading $R_{\gamma\gamma} > 1$ and $R_{\gamma\gamma} < 1$, respectively. The magnitude becomes sizable as the decreasing of the H^\pm mass since g_{H^\pm} is proportional to the $1/m_{H^\pm}^2$. For $m_2 = 90$ GeV and λ_3 in the range of -0.2 and -1.5, $R_{\gamma\gamma}$ varies from 1.1 to 1.95.

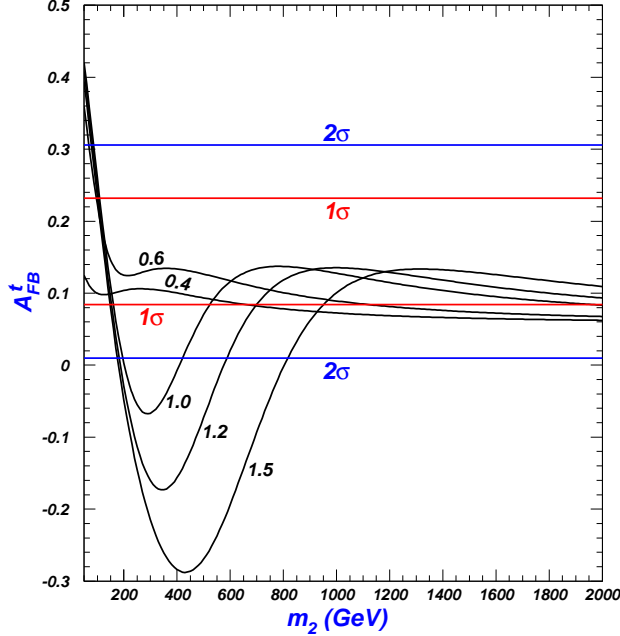


FIG. 2: The top forward-backward asymmetry A_{FB}^t at Tevatron versus m_2 for several different y_1 . The horizontal lines show the 1σ and 2σ ranges from the corresponding experimental data.

V. TOP QUARK FORWARD-BACKWARD ASYMMETRY AT TEVATRON

In the $t\bar{t}$ rest frame at Tevatron, the top quark forward-backward asymmetry A_{FB}^t is defined by [17]

$$A_{FB}^t = A_{FB}^{NP} \times R + A_{FB}^{SM} \times (1 - R) \quad (15)$$

where $A_{FB}^{SM} = 0.058$ is the asymmetry in the SM, and

$$A_{FB}^{NP} = \frac{\sigma^{NP}(\Delta y > 0) - \sigma^{NP}(\Delta y < 0)}{\sigma^{NP}(\Delta y > 0) + \sigma^{NP}(\Delta y < 0)}, \quad (16)$$

$$R = \frac{\sigma^{NP}}{\sigma^{SM} + \sigma^{NP}} \quad (17)$$

are the asymmetry induced by the new physics and the fraction of the new physics contribution to the total cross section, respectively. Δy is the rapidity difference between a top and an anti-top. In our calculations, we take $m_t = 172.5$ GeV and use the parton distribution function CTEQ6L [35] with renormalization scale and factorization scale $\mu_R = \mu_F = m_t$. We assume that the K-factors are universal, so that the QCD correction effects are canceled in the ratios of σ^{NP}/σ^{SM} and $\sigma^{NP}/(\sigma^{SM} + \sigma^{NP})$, and they are the same at LO and NLO.

The matrix elements M of the process $u(p_1)\bar{u}(p_2) \rightarrow t(k_1)\bar{t}(k_2)$, including the SM, new

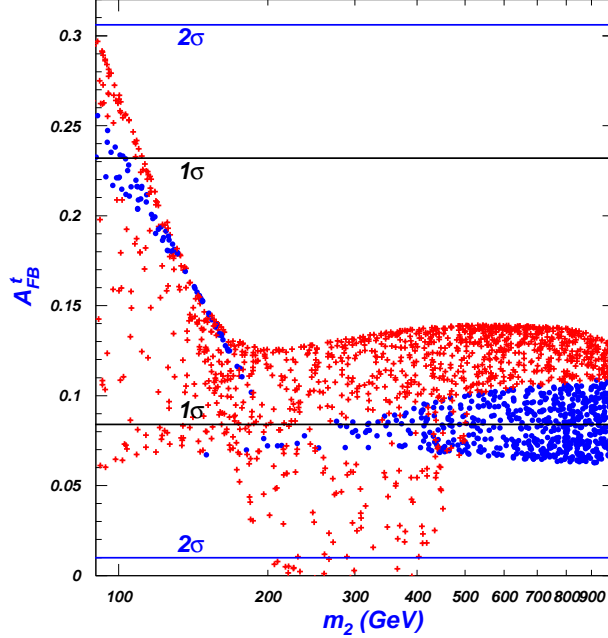


FIG. 3: The top quark forward-backward asymmetry A_{FB}^t at Tevatron versus m_2 . The bullets (blue) and crosses (red) are respectively allowed and excluded by the three experimental data of top quark. The horizontal lines show the 1σ and 2σ ranges from the corresponding experimental data.

scalar S and A contributions, can be written as ref. [20]

$$\sum |M|^2 = \frac{16g_s^4}{s^2}(t_t^2 + u_t^2 + 2sm_t^2) + 32g_s^2y^2\frac{sm_t^2 + t_t^2}{st_{m_2}} + 36\frac{y^4t_t^2}{t_{m_2}^2}, \quad (18)$$

where $s = (p_1 + p_2)^2$, $t = (p_1 - k_1)^2$, $u = (p_1 - k_2)^2$, $t_t = t - m_t^2$, $t_{m_2} = t - m_2^2$, $y = \sqrt{2}y_1$.

In Fig. 2, we plot the top quark forward-backward asymmetry A_{FB}^t at Tevatron versus the masses of S and A (m_2) for several different y_1 . We see that A_{FB}^t can be enhanced sizably for the very low value of m_2 , be over 0.1 for the large one and be negative in the intermediate region.

In Fig. 3, we scan the following parameter space,

$$0.2 \leq y_1 \leq 1.0, \quad 90 \text{ GeV} \leq m_2 \leq 1000 \text{ GeV}, \quad (19)$$

and plot A_{FB}^t versus m_2 taking into account the total decay width of top quark, top quark pair production cross section and $t\bar{t}$ mass distribution at Tevatron. We find that the relative small parameter space scanned is allowed by the above experimental data of top quark, where A_{FB}^t can be explained to within 1σ and reach 0.25. Our numerical results show that

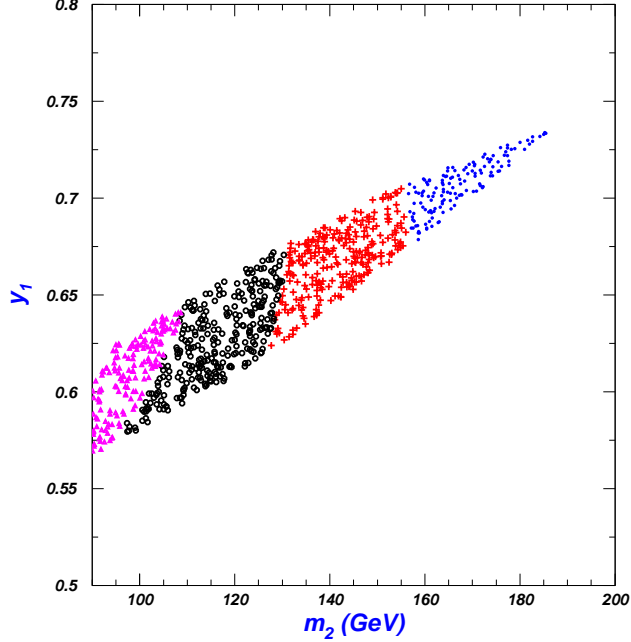


FIG. 4: Scatter plots for y_1 versus m_2 , which are allowed by the experimental data of top quark. A_{FB}^t is in the range of 0.1 – 0.14 for bullets (blue), 0.14 – 0.18 for crosses (red), 0.18 – 0.22 for circles (black) and 0.22 – 0.25 for triangle (pink), respectively.

the $t\bar{t}$ cross section and invariant mass distribution measured at Tevatron give the most constraints on the parameters y_1 and m_2 . The total top quark width can hardly give further constraints.

For the large m_2 , Fig. 3 shows A_{FB}^t is below 0.12, and Fig. 1 shows $R_{\gamma\gamma}$ is close to 1. For $m_2 < 200$ GeV, both A_{FB}^t and $R_{\gamma\gamma}$ can be enhanced sizably. Therefore, we scan

$$0.45 \leq y_1 \leq 1.0, \quad 90 \text{ GeV} \leq m_2 \leq 200 \text{ GeV}, \quad (20)$$

and give Fig. 4 and the right panel of Fig. 5. We exclude the parameters which are not in agreement with the experimental data of top quark. Fig. 4 shows the y_1 and m_2 for which A_{FB}^t can reach 0.1 – 0.25. We can see that $0.58 \leq y_1 \leq 0.7$ and $100 \text{ GeV} \leq m_2 \leq 155 \text{ GeV}$ are favored for $0.14 < A_{FB}^t < 0.22$. A very small y_1 is allowed by the experimental data of top quark, but it will lead A_{FB}^t to be much less than 0.1, which are not shown in Fig. 4.

The right frame of Fig. 5 shows m_2 versus A_{FB}^t . To examine the correlation between A_{FB}^t and the diphoton rate of the SM-like Higgs boson at LHC, we plot m_2 versus $R_{\gamma\gamma}$ for $m_h = 125$ GeV in the left panel of Fig. 5. The correlation between A_{FB}^t and $R_{\gamma\gamma}$ depends on m_2 , which can contribute to the two observables. For example, for $A_{FB}^t = 0.16$, the right

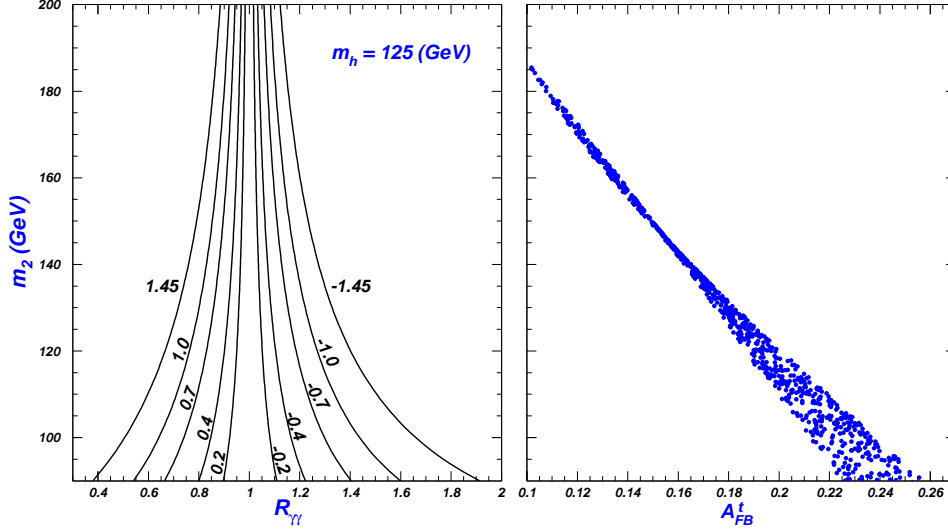


FIG. 5: The left panel: m_2 versus $R_{\gamma\gamma}$ for $m_h = 125$ GeV. The right panel: Scatter plots for m_2 versus A_{FB}^t .

panel of Fig. 5 shows that m_2 should be around 140 GeV, while, for such value of m_2 , the left panel of Fig. 5 shows that $R_{\gamma\gamma}$ is less than 1.3. By the same way, $R_{\gamma\gamma}$ should be less than 1.2 for $A_{FB}^t = 0.12$, and A_{FB}^t can reach 0.21 – 0.26 for $R_{\gamma\gamma} = 1.6$. The larger A_{FB}^t implies that the diphoton rate can be enhanced more sizably with respect to the SM prediction. Moreover, the larger $R_{\gamma\gamma}$ can imply more precisely the range of A_{FB}^t .

Note that the correlation between A_{FB}^t and $R_{\gamma\gamma}$ found in the above discussions is due to the lower bound on λ_3 coming from the requirement of vacuum stability and unitarity, and from the assumption that the scalars S , A and H^\pm are degenerate in mass. Ref. [21] shows that, for a few GeV splitting between m_S and m_A , the present experimental data of $D - \bar{D}$ mixing requires the coupling constant $y_{uc} = 2y_1(V_{CKM})^{23}$ to be smaller than 10^{-3} , i.e. $y_1 < 10^{-2}$. Therefore, the scalars S and A should be degenerate in mass so that y_1 is allowed to be enough large to explain A_{FB}^t . However, the electroweak S and T parameters allow the mass of the charged scalar to be shifted from the masses of the neutral scalars by at most ~ 110 GeV [18]. For the light scalars, the correlation between A_{FB}^t and $R_{\gamma\gamma}$ will be greatly softened and even disappear due to such mass splitting. For example, for the masses of the neutral scalars are in the range 90 – 200 GeV, the mass of the charged scalar can be as low as 90 GeV, i.e. for $0.1 < A_{FB}^t < 0.26$, the maximal value of $R_{\gamma\gamma}$ is always 1.95 (where the mass splitting gives a negligible effect on the lower bound of λ_3). Fig. 5 shows that the charged scalar and neutral scalars with less than 150 GeV mass can respectively

fit the experimental data of $R_{\gamma\gamma}$ and A_{FB}^t well. Therefore, the small mass splitting between the charged scalar and the neutral scalars is favored by the experimental data.

VI. CONCLUSION

In the framework of quasi-inert Higgs doublet model, we study the LHC diphoton rate for a SM-like Higgs boson and the top quark forward-backward asymmetry A_{FB}^t at Tevatron. Taking the theoretical and experimental constraints, we find that the diphoton rate of Higgs boson at LHC can be enhanced sizably due to the light charged Higgs contributions with respect to the SM prediction, while the measurement of the top quark forward-backward asymmetry at Tevatron can be explained to within 1σ due to the non-SM neutral Higgs bosons contributions. Besides, there are some correlations between the two observables. Compared to the SM prediction, the diphoton rate can be enhanced more sizably for the larger top quark forward-backward asymmetry. Furthermore, the range of A_{FB}^t can be narrowed more sizably for the larger $R_{\gamma\gamma}$.

Acknowledgment

This work was supported by the National Natural Science Foundation of China (NNSFC) under grant Nos. 11105116 and 11005089.

-
- [1] CMS collaboration, talk given by G. Tonelli at CERN on Dec 13 2011; ATLAS collaboration, ATLAS note ATLAS-CONF-2011-161.
 - [2] CMS collaboration, arXiv:1202.1487.
 - [3] ATLAS collaboration, arXiv:1202.1414.
 - [4] A. Djouadi, V. Driesen, W. Hollik, and Jose I. Illana, *Eur. Phys. Jour. C* **1**, 149 (1998); M. Carena, S. Gori, N. R. Shah, and C. E. M. Wagner, arXiv:1112.3336; J. Cao, Z. Heng, D. Li, J. M. Yang, arXiv:1112.4391; arXiv:1202.5821; N. Christensen, T. Han, S. Su, arXiv:1203.3207.
 - [5] P. Posch, *Phys. Lett. B* **696**, 447 (2011); G. Burdman, C. Haluch, R. Matheus, arXiv:1112.3961; N. Chen, H. J. He, arXiv:1202.3072; X.-G. He, B. Ren, J. Tandean, arXiv:1112.6364; E. Cervero, J.-M. Gerard, arXiv:1202.1973.

- [6] A. Arhrib, R. Benbrik, N. Gaur, arXiv:1201.2644.
- [7] J. Cao, Z. Heng, T. Liu, J. M. Yang, Phys. Lett. B **703**, 462 (2011); U. Ellwanger, Phys. Lett. B **698**, 293 (2011); arXiv:1112.3548.
- [8] T. Han, H. E. Logan, B. McElrath, L.-T. Wang, Phys. Lett. B **563**, 191 (2003); C. R. Chen, K. Tobe, C. P. Yuan, Phys. Lett. B **640**, 263 (2006); L. Wang, J. M. Yang, Phys. Rev. D **84**, 075024 (2011).
- [9] A. Arhrib, R. Benbrik, M. Chabab, G. Moulataka, L. Rahili, arXiv:1112.5453; P. F. Perez, H. H. Patel, M. J. Ramsey-Musolf, and K. Wang, Phys. Rev. D **79**, 055024 (2009).
- [10] G. Blanger, A. Belyaev, M. Brown, M. Kakizaki, A. Pukhov, arXiv:1201.5582; F. Goertz, U. Haisch, M. Neubert, arXiv:1112.5099; K. Cheung, T.-C. Yuan, arXiv:1112.4146.
- [11] CDF Collaboration, Phys. Rev. D **83**, 112003 (2011).
- [12] D0 Collaboration, arXiv:1107.4995.
- [13] J. H. Kuhn and G. Rodrigo, Phys. Rev. D **59**, 054017 (1999); M. T. Bowen, S. D. Ellis and D. Rainwater, Phys. Rev. D **73**, 014008 (2006); O. Antunano, J. H. Kuhn and G. Rodrigo, Phys. Rev. D **77**, 014003 (2008).
- [14] Aaltonen et al. (CDF Collaboration), Phys. Rev. D **83**, 112003 (2011).
- [15] P. Ferrario and G. Rodrigo, JHEP **1002**, 051 (2010); P. H. Frampton *et al.*, Phys. Lett. B **683**, 294 (2010); Y. Bai *et al.*, JHEP **1103**, 003 (2011); K. Kumar *et al.*, JHEP **1008**, 052 (2010); G. Burdman *et al.*, Phys. Rev. D **83**, 035012 (2011); R. Foot, Phys. Rev. D **83**, 114013 (2011); A. Djouadi *et al.*, Phys. Lett. B **701**, 458 (2011); G. M. Tavares and M. Schmaltz, arXiv:1107.0978; E. Gabrielli, M. Raidal, arXiv:1106.4553; H. Davoudiasl, T. McElmurry, A. Soni, arXiv:1108.1173; X.-P. Wang et al., Phys. Rev. D **83**, 115010 (2011); J. A. Aguilar-Saavedra, M. Perez-Victoria, Phys. Lett. B **705**, 228-234 (2011).
- [16] K. Cheung *et al.*, Phys. Lett. B **682**, 287 (2009); V. Barger *et al.*, Phys. Rev. D **81**, 113009 (2010); A. Arhrib, R. Benbrik, C. H. Chen, Phys. Rev. D **82**, 034034 (2010); J. Cao *et al.*, Phys. Rev. D **81**, 014016 (2010); Phys. Rev. D **83**, 034024 (2011); Phys. Rev. D **84**, 074001 (2011); arXiv:1109.6543; S. Jung, A. Pierce, J. D. Wells, Phys. Rev. D **83**, 114039 (2011); A. Rajaraman, Z. E. Surujon, T. M. P. Tait, arXiv:1104.0947; B. Grinstein, *et al.*, arXiv:1108.4027; M. Frank, A. Hayreter, I. Turan, arXiv:1108.0998; E. L. Berger *et al.*, Phys. Rev. Lett. **106**, 201801 (2011); Z. Ligeti, G. M. Tavares, M. Schmaltz, JHEP **1106**, 109 (2011); J. Shu, K. Wang, G. Zhu, arXiv:1104.0083; J. F. Kamenik, J. Shu, J. Zupan, arXiv:1107.5257;

- J.-Y. Liu, Y. Tang, Y.-L. Wu, arXiv:1108.5012; J. A. Aguilar-Saavedra, M. Perez-Victoria, JHEP **1109**, 097 (2011); P. Ko, Y. Omura, C. Yu, JHEP **1201**, 147 (2012); arXiv:1201.1352; B. Bhattacharjee, S. S. Biswal, D. Ghosh, Phys. Rev. D **83**, 091501 (2011); I. Dorsner, S. Fajfer, J. F. Kamenik, N. Kosnik, Phys. Rev. D **81**, 055009 (2010); M. I. Gresham, I.-W. Kim, S. Tulin, K. M. Zurek, arXiv:1203.1320; K. M. Patel and P. Sharma, JHEP **1104**, 085 (2011).
- [17] Q.-H. Cao *et al.*, Phys. Rev. **D81**, 114004 (2010).
- [18] K. Blum, Y. Hochberg, Y. Nir, JHEP **1110**, 124 (2011).
- [19] L. Wang, L. Wu, J. M. Yang, arXiv:1111.4771.
- [20] J. Shu, T. M. P. Tait, K. Wang, Phys. Rev. D **81**, 034012 (2010).
- [21] Q.-H. Cao, M. Carena, S. Gori, A. Menon, P. Schwaller, C. E. M. Wagner, L.-T. Wang, JHEP **1108**, 002 (2011).
- [22] CDF Collaboration, Phys. Rev. Lett. **106**, 171801 (2011).
- [23] D0 Collaboration, Phys. Rev. Lett. **107**, 011804 (2011).
- [24] CMS Collaboration, JHEP **1108**, 005 (2011).
- [25] DELPHI Collaboration, J. Abdallah *et al.*, Eur. Phys. Jour. C **34**, 399 (2004).
- [26] S. Nie, M. Sher, Phys. Lett. B **449**, 89 (1999); S. Kanemura, T. Kasai, Y. Okada, Phys. Lett. B **471**, 182 (1999); P. M. Ferreira, R. Santos, A. Barroso, Phys. Lett. B **603**, 219 (2004).
- [27] B. W. Lee, C. Quigg and H. B. Thacker, Phys. Rev. D **16**, 1519 (1977); R. Casalbuoni, D. Dominici, F. Feruglio R. Gatto, Nucl. Phys. B **299**, 117 (1988).
- [28] T. Aaltonen *et al.* [CDF Collaboration], CDF note 9913.
- [29] U. Langenfeld, S. Moch, P. Uwer, Phys. Rev. D **80**, 054009 (2009).
- [30] V. Ahrens, *et al.*, JHEP **1009**, 097 (2010).
- [31] CDF Collaboration], Phys. Rev. Lett. **102**, 222003 (2009).
- [32] V. M. Abazov *et al.* [D0 Collaboration], Phys. Rev. Lett. **106**, 022001 (2011).
- [33] D0 Collaboration, Phys. Lett. B **705**, 313 (2011).
- [34] A. Djouadi, Phys. Rept. **459**, 1 (2008).
- [35] J. Pumplin *et al.*, JHEP **0602**, 032 (2006).